

## Carbon and silicon vacancies in electron-irradiated 6H-SiC

S. Dannefaer, D. Craigen, and D. Kerr

Department of Physics, University of Winnipeg, Winnipeg, Manitoba, Canada R3B 2E9

(Received 4 August 1994)

Positron-lifetime and Doppler-broadening spectroscopies were used to investigate vacancies formed by 2.2- and 10-MeV electrons. Carbon vacancies yield a positron lifetime of 160 ps, only 15 ps longer than the bulk lifetime, and the Doppler-broadening  $S$  parameter is very close to that for the bulk. For silicon vacancies the positron lifetime is 260 ps and the  $S$  parameter is 1.12 times the bulk value. In  $n$ -type materials the defects are neutral, whereas in  $p$ -type materials no vacancies are detected. Introduction rates of carbon and silicon vacancies were also determined.

With the advent of high-quality SiC substrates there is now considerable interest in this material for electronic devices and characterization of defects is therefore of importance. In this work we have investigated vacancies formed by electron irradiation of 6H-SiC single crystals. The detection of the vacancies was done by positron lifetime and Doppler-broadening measurements, the aim being to establish the characteristic positron responses for specific defects. Several positron measurements have already been done,<sup>1-4</sup> but unfortunately it was not possible to conduct a full decomposition of lifetime data.<sup>1,2</sup> Electron paramagnetic resonance investigations on 3C-SiC suggest formation of the silicon vacancy<sup>5</sup> and in  $p$ -type material only, the positively charged carbon vacancy.<sup>6</sup>

The positron lifetime spectrometer had a time resolution of 180 ps (full width at half maximum) and each spectrum was accumulated to a total of  $8 \times 10^6$  counts with most of the spectra being repeated three times. Doppler-broadening spectra were accumulated to a total of  $2 \times 10^6$  counts in the Doppler-broadened annihilation peak and each measurement was repeated five times. The energy resolution was 1.2 at 511 keV. The irradiation was done using a pulsed beam (240 pulses/s each of duration 3  $\mu$ s). The average current density was 5  $\mu$ A/cm<sup>2</sup>, and the samples were watercooled directly. The samples were of two types:  $n$ -type ( $N$ -doped) with  $6 \times 10^{17}$  carriers/cm<sup>3</sup> (research grade from Cree Research) and  $p$ -type with  $7 \times 10^{18}$  carriers/cm<sup>3</sup> (production grade).

Table I gives the results for unirradiated samples as well as an irradiated  $p$ -type sample. The lifetime spectra are characterized by a dominant  $\tau_1$  lifetime with an intensity ( $I_1$ ) of 94% or more. The much longer lived  $\tau_2$  component is weak but does not arise from the positron source itself since using a directly deposited weak (2  $\mu$ Ci)

positron source, no change was observed. This component was therefore included to calculate the bulk lifetime,  $\tau_B$ , according to the simple trapping model,<sup>7</sup> yielding a value of 144 ps. Girka *et al.*<sup>1</sup> found a somewhat higher value (157 ps); both values fall well inside the theoretically estimated range of 134 to 163 ps.<sup>8</sup>

For the unirradiated samples no temperature effects (down to 30 K) could be found, indicating absence of shallow positron traps. These samples contain only few ( $\approx 10^{16}$ /cm<sup>3</sup>) vacancy clusters. For the irradiated  $p$ -type sample this too was the case and, furthermore, illumination with white light (at 30 K) was not effective in making observable any irradiation-produced vacancies.

The  $S$  parameter is also unaffected by conductivity type as well as irradiation. Its value of 0.4193 can, in view of the lifetime data, therefore be taken to represent the bulk value  $S_B$ , which is characteristic of the electron momentum distribution in 6H-SiC.  $S_B$  is, as expected, significantly lower than that for float-zone silicon which in our case has a value of 0.4863.

For the electron irradiated  $n$ -type material lifetime and Doppler data are shown in Fig. 1 as a function of dose (note that 2.2-MeV electrons were used for doses  $\leq 6 \times 10^{17}$ /cm<sup>2</sup> while 10-MeV electrons were used for the  $12 \times 10^{17}$ /cm<sup>2</sup> dose). The  $S$  parameter (panel *A*) as well as the average lifetime,  $\langle \tau \rangle$  (panel *B*), defined as  $I_1\tau_1 + I_2\tau_2 + I_3\tau_3$ , both already show saturation after a dose of  $2 \times 10^{17}$ /cm<sup>2</sup>. For the sake of comparison the average lifetime for 4-MeV electron-irradiated 6H-SiC according to Girka *et al.*<sup>1</sup> is also shown. Their data also show saturation and the level is intermediate between our 2.2 and 10-MeV high-dose data points. Therefore, the  $S$ -parameter data and  $\langle \tau \rangle$  both show that at doses above  $2 \times 10^{17}$ /cm<sup>2</sup> all positrons have become trapped by vacan-

TABLE I. Positron lifetime and Doppler results for unirradiated samples and for a  $1.2 \times 10^{18}$ /cm<sup>2</sup> 10-MeV irradiated  $p$ -type sample.

6H-SiC	$\tau_1$ (ps)	$\tau_2$ (ps)	$I_1$ (%)	$I_2$ (%)	$\tau_B$ (ps)	$S$ ( $\pm 0.0005$ )
$n$ type	140 $\pm$ 2	300 $\pm$ 10	94 $\pm$ 1	6 $\pm$ 1	144 $\pm$ 1	0.4193
$p$ type	141 $\pm$ 2	343 $\pm$ 10	96.5 $\pm$ 0.5	3.5 $\pm$ 0.5	144 $\pm$ 2	0.4193
$p$ type Irradiated	141 $\pm$ 1	360 $\pm$ 10	97.3 $\pm$ 0.5	2.7 $\pm$ 0.5	143 $\pm$ 2	0.4193

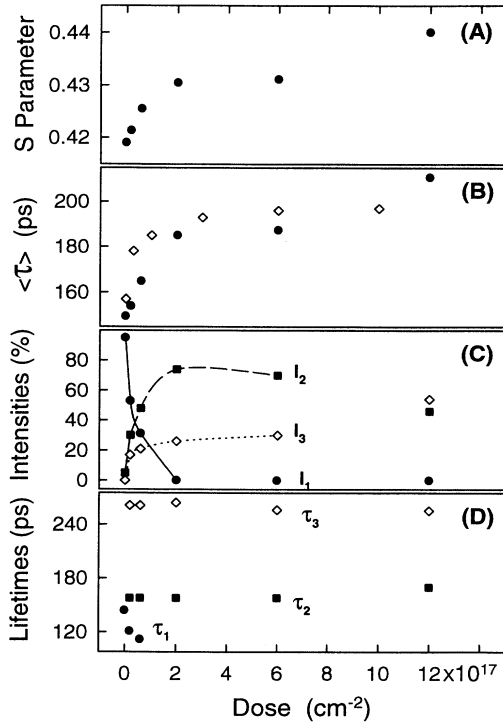


FIG. 1. Lifetime and Doppler data for *n*-type 6H-SiC as a function of dose. For doses  $\leq 6 \times 10^{17}/\text{cm}^2$  the electron energy was 2.2 MeV. For the  $12 \times 10^{17}/\text{cm}^2$  dose the energy was 10 MeV. Open diamonds in panel (B) are from Ref. 1 and correspond to an electron energy of 4 MeV. In panels (C) and (D) the individual intensities and lifetimes are shown.

cies. From the decomposed lifetime data [panels (C) and (D)] two lifetimes can be resolved, one at 160 and the other at 260–270 ps. The intensity of the 260–270 ps component is close to 28% for the electron energy of 2.2 MeV, whereas it is 45% for 10 MeV. This suggests that independent of electron energy two vacancy types have been created but that the balance between these two defects is energy dependent. Since we have complete trapping, the intensities of the 160- and the 260–270-ps lifetime components express the fraction of positrons being trapped by the two vacancy types. The lifetime data can be combined with the Doppler data with the aim of establishing the *S* parameter values characteristic for the two vacancy types. With complete trapping, the *S* parameter contains no contribution from the bulk of the sample so that *S* may be expressed as the sum of the two vacancy contributions

$$S(E_{\text{irr}}) = I_{160}S_{160} + I_{260}S_{260}, \quad (1)$$

where  $I_{160} (= 1 - I_{260})$  is the intensity of the 160-ps life-

time component and  $S_{160}$  is the characteristic *S* parameter arising from positrons trapped by this vacancy type (like definition for  $S_{260}$ ). Since  $S(E_{\text{irr}})$  is known for both 2.2 and 10 MeV there are two equations to determine these characteristic *S* parameters and we find  $S_{160} \approx 0.416$  and  $S_{260} \approx 0.470$  (both with uncertainty  $\pm 0.002$ ). Since the bulk value of *S* is 0.4193 (see Table I), this means that  $S_{160}$  is essentially equal to  $S_B$  whereas  $S_{260}$  is 12% larger. Hence, the defect which gives rise to the 160-ps lifetime is essentially “invisible” in Doppler-broadening experiments.

For the lesser irradiated ( $2$  and  $6 \times 10^{16}/\text{cm}^2$ ) samples the lifetime data show incomplete trapping because of the existence of a short-lived component  $\tau_1$ , whose value decreases from 141 ps [see panel (D), Fig. 1] and whose intensity decreases from 94% with increasing dose. Calculating the bulk lifetime based on these fits gave 140–150 ps in good agreement with the bulk lifetime listed in Table I, so it is now possible to calculate the trapping rates corresponding to the two vacancy-related lifetimes (see Table II). In the case of incomplete trapping the *S* parameter also contains a contribution from the bulk of the sample in addition to the two vacancy contributions

$$S = (1 - f_{160} - f_{260})S_B + f_{160}S_{160} + f_{260}S_{260}. \quad (2)$$

Here  $f_{160}$  (and similarly for  $f_{260}$ ) is given by

$$f_{160} = \frac{\kappa_{160}}{\kappa_{160} + \lambda_B}, \quad (3)$$

where  $\kappa_{160}$  is the trapping rate calculated from the lifetime data using the simple trapping model [note that Eq. (1) is just a special case of Eq. (2) for which  $f_{160} = I_{160}$ ,  $f_{260} = I_{260}$ , and  $I_{160} + I_{260} = 1$ ]. From Table I we have  $\lambda_B \equiv 1/\tau_B = 6.95 \text{ ns}^{-1}$ , and using the above-mentioned values for  $S_B$ ,  $S_{160}$  and  $S_{260}$  plus the trapping rates, one can calculate the *S* value ( $S_{\text{calc}}$ ) and compare with the experimental value from panel (A) in Fig. 1. The results are listed in Table II, from which we can conclude that the  $S_{160}$  and the  $S_{260}$  values deduced from the case of complete trapping also give satisfactory results when applied to the case of incomplete trapping.

It is worth noting that in a recent Doppler-broadening investigation on a  $30\text{-}\mu\text{m}$  thick 3C-SiC epitaxially grown (on Si) layer using slow positrons, Itoh *et al.*<sup>4</sup> found a much weaker increase in *S* with the dose of 1 MeV electrons. One explanation might be that this low energy creates much fewer of the vacancies which give a detectable deviation from the bulk, i.e.,  $S_{260}$ .

The most likely physical interpretation of the two vacancy-related lifetime components is that the 160-ps lifetime arises from positrons trapped at carbon vacancies

TABLE II. Trapping rates associated with the 160- and 260-ps lifetimes for lightly irradiated *n*-type samples and calculated *S* parameters as compared to experimental values.

Dose (2.2 MeV)	$\kappa_{160}$ ( $\text{ns}^{-1}$ )	$\kappa_{260}$ ( $\text{ns}^{-1}$ )	$S_{\text{calc}}$	$S_{\text{exp}}$
$2 \times 10^{16}/\text{cm}^2$	$0.7 \pm 0.2$	$0.7 \pm 0.2$	$0.423 \pm 0.002$	$0.4213 \pm 0.0005$
$6 \times 10^{16}/\text{cm}^2$	$1.25 \pm 0.1$	$1.03 \pm 0.1$	$0.425 \pm 0.002$	$0.4263 \pm 0.0005$

TABLE III. Introduction rates for carbon ( $\eta_C$ ) and silicon vacancies ( $\eta_{Si}$ ) and the ratio between vacancy concentrations. The entry at 4 MeV was calculated from the data of Girka *et al.* (Ref. 1) NC stands for noncalculable.

Dose ( $\times 10^{16}/\text{cm}^2$ )	Electron energy (MeV)	$\eta_C$ ( $\text{cm}^{-1}$ )	$\eta_{Si}$ ( $\text{cm}^{-1}$ )	$[V_C]/[V_{Si}]$
2	2.2	3.5	3.5	1.0
6	2.2	2.0	1.6	1.3
20	2.2	NC	NC	2.4
60	2.2	NC	NC	2.3
> 60	4	NC	NC	1.5
120	10	NC	NC	1.2

(the monovacancy in diamond yields a value close to 150 ps)<sup>9</sup> while the 260-ps lifetime arises from positrons trapped at silicon vacancies (in silicon the monovacancy yields 270 ps).<sup>10</sup> Theoretical calculations<sup>8</sup> suggest that the silicon vacancy should yield a lifetime of 249 ps according to the semiempirical insulator model but also that carbon vacancies should *not* be a positron trap. Considering that the carbon vacancy proposed here only represents a 10% increase over the bulk lifetime, such a small increase might well be inaccessible to theoretical calculations.

Neither of the vacancy types observed in the *n*-type material were detected in the *p*-type material (see Table I). This can arise from two causes: The first is that the vacancies may be positively charged and therefore unable to trap positrons. This is a distinct possibility since Itoh *et al.*<sup>6</sup> detect a paramagnetic resonance signal (*T*5), which they ascribe to a positively charged carbon vacancy, only in *p*-type 3C-SiC. Secondly, the introduction rate of vacancies may be much smaller in *p*-type materials (and ours is strongly *p*-type) than in *n*-type, since type dependency on irradiation damage is commonly observed for semiconductors. The vacancies we do observe in *n*-type material appear to be neutral since no change in the *S* parameter with temperature (down to 30 K) was found for the  $6 \times 10^{16}/\text{cm}^2$  irradiated sample.

Based on the trapping rates listed in Table II, where  $\kappa_{160}$  and  $\kappa_{260}$  represent the trapping rate for neutral  $V_C$  and  $V_{Si}$ , respectively, we can estimate the concentrations of these defects since trapping rates are proportional to concentrations. This estimation is based on the assumption that a trapping rate of  $1 \text{ ns}^{-1}$  corresponds to a concentration of  $10^{17}/\text{cm}^3$  on *each* sublattice. This “conversion” factor is well established in the case of diamond,<sup>9</sup>

silicon,<sup>11</sup> and GaAs<sup>12</sup> when taking into account the different number density of atoms for the various materials. Furthermore, the ratio between the carbon and silicon vacancy concentrations can be found and this calculation can be extended also to high doses where complete trapping occurs (absolute concentrations, however, are not calculable). The results are shown in Table III, in which the estimated ratio is also included for the 4-MeV irradiated high-dose data of Girka *et al.*<sup>1</sup> It is evident that the introduction rates on each sublattice initially are high and about the same. The decrease in the introduction rate and, in particular, a systematic increase with a dose of the  $[V_C]/[V_{Si}]$  concentration ratio for the 2.2-MeV irradiations suggests that “secondary” effects become observable, possibly arising from a *net* conversion of silicon vacancies to carbon vacancies plus associated antisites. Such an effect might well be particle energy dependent, as suggested by the systematic decrease in the  $[V_C]/[V_{Si}]$  ratio with increasing energy at high doses.

In conclusion, we have presented positron lifetime and Doppler-broadening data on electron-irradiated 6H-SiC which show that both neutral carbon and silicon vacancies are formed in *n*-type materials, but in *p*-type materials no vacancy responses could be found. The vacancy introduction rates are initially large ( $\sim 3.5 \text{ cm}^{-1}$  on each sublattice) but the balance between the vacancy concentrations changes in favor of carbon vacancies with increasing dose. With increasing electron energy equipartition between the vacancy concentrations is approached at 10 MeV.

This work was financially assisted by the Natural Sciences and Engineering Research Council of Canada.

- <sup>1</sup>A. I. Girka, V. A. Kuleshin, A. D. Mokrushin, E. N. Mokhov, S. V. Svirida, and A. V. Shishkin, *Fiz. Tekh. Poluprovodn.* **23**, 2159 (1989) [*Sov. Phys. Semicond.* **23**, 1337 (1989)].  
<sup>2</sup>A. I. Girka, A. D. Mokrushin, E. N. Mokhov, V. M. Osadchiv, S. V. Svirida, and A. V. Shishkin, *Zh. Eksp. Teor. Fiz.* **97**, 578 (1990) [*Sov. Phys. JETP* **70**, 322 (1990)].  
<sup>3</sup>H. Itoh, M. Yoshikawa, I. Nashiyama, L. Wei, S. Tanigawa, S. Misawa, H. Okumura, and S. Yoshida, *Mater. Sci. Forum* **117-118**, 501 (1993).  
<sup>4</sup>H. Itoh, M. Yoshikawa, I. Nashiyama, L. Wei, S. Tanigawa, S. Misawa, H. Okumura, and S. Yoshida, *Hyperfine Interact.* **79**, 725 (1993).  
<sup>5</sup>H. Itoh, N. Hayakawa, I. Nashiyama, and E. Sakuma, *J. Appl.*

- Phys.* **66**, 4529 (1989).  
<sup>6</sup>H. Itoh, M. Yoshikawa, I. Nashiyama, S. Misawa, H. Okumura, and S. Yoshida, *J. Electron. Mater.* **21**, 707 (1992).  
<sup>7</sup>R. N. West, *Adv. Phys.* **22**, 263 (1973).  
<sup>8</sup>M. J. Puska, S. Mäkinen, M. Manninen, and R. M. Nieminen, *Phys. Rev. B* **39**, 7666 (1989).  
<sup>9</sup>S. Dannefaer, P. Mascher, and D. Kerr, *Diamond Relat. Mater.* **1**, 407 (1992).  
<sup>10</sup>S. Dannefaer, *Phys. Status Solidi A* **102**, 481 (1987).  
<sup>11</sup>P. Mascher, S. Dannefaer, and D. Kerr, *Phys. Rev. B* **40**, 11 764 (1989).  
<sup>12</sup>S. Dannefaer and D. Kerr, *Phys. Rev. B* **48**, 9142 (1993).